

Summertime ozone formation in Xi'an and surrounding areas, China

T. Feng et al.

This discussion paper is/has been under review for the journal Atmospheric Chemistry and Physics (ACP). Please refer to the corresponding final paper in ACP if available.

# Summertime ozone formation in Xi'an and surrounding areas, China

T. Feng<sup>1,2,3</sup>, N. Bei<sup>1,2</sup>, R. Huang<sup>2,4</sup>, J. Cao<sup>2,3</sup>, Q. Zhang<sup>5</sup>, W. Zhou<sup>3</sup>, X. Tie<sup>2,3</sup>, S. Liu<sup>2,3</sup>, T. Zhang<sup>2,3</sup>, X. Su<sup>2,3</sup>, W. Lei<sup>6</sup>, L. T. Molina<sup>6</sup>, and G. Li<sup>2,3</sup>

<sup>1</sup>School of Human Settlements and Civil Engineering, Xi'an Jiaotong University, Xi'an, China

<sup>2</sup>Key Laboratory of Aerosol Chemistry and Physics, Institute of Earth Environment, Chinese Academy of Sciences, Xi'an, China

<sup>3</sup>State Key Laboratory of Loess and Quaternary Geology, Institute of Earth Environment, Chinese Academy of Sciences, Xi'an, China

<sup>4</sup>Laboratory of Atmospheric Chemistry, Paul Scherrer Institute (PSI), Villigen, Switzerland

<sup>5</sup>Department of Environmental Sciences and Engineering, Tsinghua University, Beijing, China

<sup>6</sup>Molina Center for Energy and the Environment, La Jolla, CA, USA

Received: 3 June 2015 – Accepted: 20 October 2015 – Published: 4 November 2015

Correspondence to: G. Li (ligh@ieecas.cn)

Published by Copernicus Publications on behalf of the European Geosciences Union.

Title Page

Abstract

Introduction

Conclusions

References

Tables

Figures

◀

▶

◀

▶

Back

Close

Full Screen / Esc

Printer-friendly Version

Interactive Discussion



## Abstract

In the study, the ozone ( $O_3$ ) formation is investigated in Xi'an and surrounding areas, China using the WRF-CHEM model during the period from 22 to 24 August 2013 corresponding to a heavy air pollution episode with high concentrations of  $O_3$  and  $PM_{2.5}$  (particulate matter with aerodynamic diameter less than  $2.5\ \mu\text{m}$ ). The WRF-CHEM model generally performs well in simulating the surface temperature and relative humidity compared to the observations and also reasonably reproduces the observed temporal variations of the surface wind speed and direction. The convergence formed in Xi'an and surrounding areas is favorable for the accumulation of pollutants, causing high concentrations of  $O_3$  and  $PM_{2.5}$ . In general, the calculated spatial patterns and temporal variations of near-surface  $O_3$  and  $PM_{2.5}$  are consistent well with the measurement at the ambient monitoring stations. The simulated daily mass concentrations of aerosol constituents, including sulfate, nitrate, ammonium, elemental and organic carbon, are also in good agreement with the filter measurements. High aerosol concentrations in Xi'an and surrounding areas significantly decrease the photolysis frequencies and can reduce near-surface  $O_3$  concentrations by more than  $50\ \mu\text{g m}^{-3}$  (around 25 ppb) on average. Sensitivity studies show that the  $O_3$  production regime in Xi'an and surrounding areas is complicated, varying from  $\text{NO}_x$  to VOC-sensitive chemistry. The industry emissions contribute the most to the  $O_3$  concentrations compared to the natural and other anthropogenic sources, but still do not play a determined role in the  $O_3$  formation. The complicated  $O_3$  production regime and high aerosol levels constitute a dilemma for  $O_3$  control strategies in Xi'an and surrounding areas. In the condition with high  $O_3$  and  $PM_{2.5}$  concentrations, decreasing various anthropogenic emissions cannot efficiently mitigate the  $O_3$  pollution, and a 50 % reduction of all the anthropogenic emissions only decreases near-surface  $O_3$  concentrations by less than 14 % during daytime. Further studies need to be performed for  $O_3$  control strategies considering manifest changes of the emission inventory and uncertainties of meteorological field simulations.

## Summertime ozone formation in Xi'an and surrounding areas, China

T. Feng et al.

Title Page

Abstract

Introduction

Conclusions

References

Tables

Figures



Back

Close

Full Screen / Esc

Printer-friendly Version

Interactive Discussion



## 1 Introduction

Ozone (O<sub>3</sub>) is a key species in the atmosphere due to its controlling role in the photochemistry in the stratosphere and troposphere (Seinfeld and Pandis, 2006) since O<sub>3</sub> and its photochemical derivative, OH, are the key oxidants for most reduced gases (Brasseur et al., 1999). Atmospheric O<sub>3</sub> also contributes to the global climate change because of absorption of the infrared radiation, constituting one of the important short-lived climate pollutants. Additionally, high levels of surface O<sub>3</sub> exert deleterious impacts on ecosystems and human health (Cao et al., 2012; Zhou et al., 2011) and thence O<sub>3</sub> becomes one of the criteria pollutants regulated by the environmental agencies in many countries, such as US Environmental Protection Agency (US EPA) and the China's Ministry of Environmental Protection (China MEP).

Rapid industrialization and urbanization have caused severe air pollution recently in China (e.g., De Smedt et al., 2010; Lu et al., 2011) and numerous studies have been performed to investigate the severe O<sub>3</sub> pollution, particularly in the Beijing–Tianjin–Hebei region (e.g., Wang et al. 2006; Lin et al., 2008; Tang et al., 2009; Xu et al., 2011), Yangtze Delta region (e.g., Geng et al., 2009, 2011; Tie et al., 2009, 2012), and Pearl River Delta region (e.g., Zhang et al., 2008; T. Wang et al., 2009; Cheng et al., 2010; Wang et al., 2011; Li et al., 2013). For example, T. Wang et al. (2006) have observed strong O<sub>3</sub> production in urban plumes from Beijing with a maximum O<sub>3</sub> concentration of 286 ppb. Using a chemical transport model, Tie et al. (2009) have shown that unfavorable meteorological conditions cause high near-surface O<sub>3</sub> level exceeding 100 ppb in the Shanghai region. T. Wang et al. (2009) have reported increasing surface O<sub>3</sub> concentrations in the background atmosphere of Southern China during the period from 1994 to 2007.

As the largest city in northwestern China with the population of more than 8 million, Xi'an is located in the Guanzhong basin. The basin is nestled between the Qinling Mountains in the south and the Loess Plateau in the north, with a warm-humid climate. The unique topography is not favorable for the dispersion of air pollutants (Fig. 1a)

ACPD

15, 30563–30608, 2015

### Summertime ozone formation in Xi'an and surrounding areas, China

T. Feng et al.

Title Page

Abstract

Introduction

Conclusions

References

Tables

Figures



Back

Close

Full Screen / Esc

Printer-friendly Version

Interactive Discussion





## 2 Model and method

### 2.1 WRF-CHEM model

In this study, a specific version of the WRF-CHEM model (Grell et al., 2005) is applied to verify the O<sub>3</sub> formation in Xi'an and surrounding areas, which is developed by Li et al. (2010, 2011a, b, 2012) at the Molina Center for Energy and the Environment, with a new flexible gas phase chemical module and the CMAQ (version 4.6) aerosol module developed by US EPA (Binkowski and Roselle, 2003). The wet deposition follows the method used in the CMAQ and the dry deposition of chemical species is parameterized following Wesely (1989). The photolysis rates are calculated using the FTUV (Tie et al., 2003; Li et al., 2005) in which the impacts of aerosols and clouds on the photochemistry are considered (Li et al., 2011a).

We utilize ISORROPIA Version 1.7 (<http://nenes.eas.gatech.edu/ISORROPIA/>) to simulate the inorganic aerosols in the WRF-CHEM model. The inorganic aerosol module calculates the composition and phase state of an ammonium-sulfate-nitrate-chloride-sodium-calcium-potassium-magnesium-water inorganic aerosol in thermodynamic equilibrium with gas phase precursors. In the present study, the module is primarily used to predict the thermodynamic equilibrium between the ammonia-sulfate-nitrate-chloride-water aerosols and their gas phase precursors of H<sub>2</sub>SO<sub>4</sub>-HNO<sub>3</sub>-NH<sub>3</sub>-HCl-water vapor.

The secondary organic aerosol (SOA) formation is predicted using a non-traditional SOA module. The module includes the volatility basis-set (VBS) modeling method in which primary organic components are assumed to be semi-volatile and photochemically reactive and are distributed in logarithmically spaced volatility bins (Li et al., 2011b). Nine surrogate species with saturation concentrations from 10<sup>-2</sup> to 10<sup>6</sup> μg m<sup>-3</sup> at room temperature are used for the primary organic aerosol (POA) components following the approach of Shrivastava et al. (2008). Detailed description about the volatility basis-set approach can be found in Li et al. (2011b). The contributions of glyoxal and methylglyoxal to the SOA formation are also included in the SOA module. The SOA

## Summertime ozone formation in Xi'an and surrounding areas, China

T. Feng et al.

Title Page

Abstract

Introduction

Conclusions

References

Tables

Figures



Back

Close

Full Screen / Esc

Printer-friendly Version

Interactive Discussion



formation from glyoxal and methylglyoxal is parameterized as a first-order irreversible uptake by aerosol particles, with a reactive uptake coefficient of  $3.7 \times 10^{-3}$  for glyoxal and methylglyoxal (Zhao et al., 2006; Volkamer et al., 2007).

## 2.2 Model configuration

5 A three-day episode from 22 to 24 August 2013 is selected in the study, representing a heavy air pollution event in Xi'an and surrounding areas with high levels of  $O_3$  and  $PM_{2.5}$ . The WRF-CHEM model is configured with grid spacing of 3 km ( $201 \times 201$  grid points) centered at  $34.25^\circ N$  and  $109^\circ E$  (Fig. 1a). Thirty-five vertical levels are used in a stretched vertical grid with spacing ranging from 50 m near the surface,  
10 to 500 m at 2.5 km a.g.l. and 1 km above 14 km. The modeling system employs the microphysics scheme of Lin et al. (1983), the MYJ TKE planetary boundary layer scheme (Janjic, 2002), the MYJ surface layer scheme (Janjic, 2002), the Unified Noah land-surface model (Chen and Dudhia, 2000), the RRTM longwave radiation parameterization (Mlawer et al., 1997), and the Goddard shortwave module (Chou and Suarez, 1994). Meteorological initial and boundary conditions are obtained from NCEP  
15  $1^\circ \times 1^\circ$  reanalysis data. Chemical initial and boundary conditions are interpolated from MOZART 6-h output (Horowitz et al., 2003). For the episode simulations, the spin-up time of the WRF-CHEM model is one day.

The SAPRC 99 chemical mechanism is utilized in simulations. The anthropogenic emission inventory (EI) used in the present study is developed by Q. Zhang et al. (2009), including contributions from agriculture, industry, power, residential and transportation sources (Fig. 2). High emissions of volatile organic compounds (VOCs) and nitrogen oxide ( $NO_x$ ) are concentrated in Xi'an and surrounding areas. The primary organic aerosol emissions are redistributed following the study of Tsimpidi et al. (2010).  
20 Additionally, the biogenic emissions are calculated on-line with the WRF-CHEM model using the MEGAN model (Guenther et al., 2006).  
25

## Summertime ozone formation in Xi'an and surrounding areas, China

T. Feng et al.

Title Page

Abstract

Introduction

Conclusions

References

Tables

Figures



Back

Close

Full Screen / Esc

Printer-friendly Version

Interactive Discussion





















## Summertime ozone formation in Xi'an and surrounding areas, China

T. Feng et al.

Title Page

Abstract

Introduction

Conclusions

References

Tables

Figures



Back

Close

Full Screen / Esc

Printer-friendly Version

Interactive Discussion



emissions by 50 % in the WRF-CHEM simulations. Figure 14 shows the comparison of near-surface  $O_3$  concentrations averaged in the urban area of Xi'an in the reference simulation to the two sensitivity studies in which AVOCs and  $NO_x$  are decreased by 50 %, respectively. A 50 % reduction of AVOCs decreases the  $O_3$  concentration averaged in Xi'an surrounding areas consistently during the episode, particularly during peak time (defines as 14:00–16:00 BJT hereafter). A 50 % reduction of  $NO_x$  enhances the near-surface  $O_3$  level in the morning due to the emission decrease of NO, but in the afternoon, it decreases the near-surface  $O_3$  level, same as the effect from a 50 % reduction of AVOCs, leading to a complicated  $O_3$  production regime.

Figure 15a shows the 3-day average near-surface  $O_3$  change during peak time with a 50 % reduction in  $NO_x$  emissions (defined as  $O_3(\text{SEN}) - O_3(\text{REF})$ ). In the Xi'an and surrounding areas, except the urban center, the simulated average near-surface  $O_3$  concentrations are decreased by about 10–40  $\mu\text{g m}^{-3}$  due to a 50 % reduction of  $NO_x$ . The near-surface  $O_3$  concentrations are only enhanced in the urban center of Xi'an with very high  $NO_x$  emissions, but less than 10  $\mu\text{g m}^{-3}$ . A 50 % reduction of AVOCs emissions consistently reduces the near-surface  $O_3$  concentration in Xi'an and surrounding areas by up to 40  $\mu\text{g m}^{-3}$  (Fig. 15b). Apparently, the response of  $O_3$  change to a 50 % reduction of  $NO_x$  or AVOCs emissions cannot obviously indicate the  $O_3$  production regime in Xi'an and surrounding areas. Sillman (1995) proposed that the ratio of the production rates of hydrogen peroxide and nitric acid ( $H_2O_2/HNO_3$ ) can be used to investigate VOC- $NO_x$  sensitive photochemistry. If the ratio is less than 0.3, the  $O_3$  production regime is VOC sensitivity. If the ratio exceeds 0.5, the regime is  $NO_x$  sensitivity. The ratio ranging from 0.3 to 0.5 indicates the transition from  $NO_x$  to VOC-sensitive chemistry. Figure 15c displays the distribution of the 3-day average  $H_2O_2/HNO_3$  during the  $O_3$  peak time. In Xi'an and surrounding areas, the  $H_2O_2/HNO_3$  ratio varies from 0.2 to 1.0, showing that the  $O_3$  production regime is very complicated. In the south of Xi'an and surrounding areas, the  $O_3$  production regime lies in the transition from  $NO_x$  to VOC-sensitive chemistry. The analyses using  $H_2O_2/HNO_3$  indicator and the results



## Summertime ozone formation in Xi'an and surrounding areas, China

T. Feng et al.

Title Page

Abstract

Introduction

Conclusions

References

Tables

Figures



Back

Close

Full Screen / Esc

Printer-friendly Version

Interactive Discussion



$\text{O}_3$  contribution from the transportation emissions ranges from 10 to  $20 \mu\text{g m}^{-3}$  in the afternoon, and the residential emissions play a nonnegligible role in the  $\text{O}_3$  formation, with the near-surface  $\text{O}_3$  contribution less than  $10 \mu\text{g m}^{-3}$ .

Sensitivity studies have shown that there is no an individual anthropogenic emission source which dominates the  $\text{O}_3$  level in Xi'an and surrounding areas. The simulation without the most important industry source still predicts high near-surface  $\text{O}_3$  concentrations in Xi'an and surrounding areas (Fig. 17a). The  $\text{O}_3$  production regime in Xi'an and surrounding areas varies from  $\text{NO}_x$  to VOC-sensitive chemistry, constituting one of the possible reasons for the insensitivity of  $\text{O}_3$  concentration to the emission change. Additionally, in case of high aerosol levels, aerosol effects on photolysis also compensate the  $\text{O}_3$  decrease through enhancing photolysis frequencies due to decrease of aerosol concentrations caused by the emission reduction. Although the biogenic emission does not play a key role in the  $\text{O}_3$  formation in Xi'an and surrounding areas, it still provides reactive VOCs to precipitate the  $\text{O}_3$  formation. Therefore, under the situation with high  $\text{O}_3$  and  $\text{PM}_{2.5}$  in Xi'an and surrounding areas, decreasing emissions from various anthropogenic sources cannot efficiently mitigate the  $\text{O}_3$  pollution. Sensitivity studies have been performed to further demonstrate the difficulties in devising  $\text{O}_3$  control strategies through decreasing anthropogenic emissions from industry, residential, transportation, and all the anthropogenic sources by 50 %, respectively in the WRF-CHEM simulations. A 50 % reduction of the industry emissions only cause less than 7 % decrease of near-surface  $\text{O}_3$  concentrations in Xi'an and surrounding areas (Fig. 18). Even all the anthropogenic emissions are reduced by 50 %, the decrease of near-surface  $\text{O}_3$  concentrations is not more than 14 %.

## 4 Summaries and conclusions

In the study, a 3-day episode with high  $\text{O}_3$  and  $\text{PM}_{2.5}$  concentrations from 22 to 24 August 2013, is simulated using the WRF-CHEM model to verify the  $\text{O}_3$  formation in Xi'an and surrounding areas, China. The simulated surface temperatures are in good agree-







Sciences. Naifang Bei is supported by the National Natural Science Foundation of China (no. 41275101).

## References

- 5 Bei, N., de Foy, B., Lei, W., Zavala, M., and Molina, L. T.: Using 3DVAR data assimilation system to improve ozone simulations in the Mexico City basin, *Atmos. Chem. Phys.*, 8, 7353–7366, doi:10.5194/acp-8-7353-2008, 2008.
- Bei, N., Lei, W., Zavala, M., and Molina, L. T.: Ozone predictabilities due to meteorological uncertainties in the Mexico City basin using ensemble forecasts, *Atmos. Chem. Phys.*, 10, 6295–6309, doi:10.5194/acp-10-6295-2010, 2010.
- 10 Bei, N., Li, G., and Molina, L. T.: Uncertainties in SOA simulations due to meteorological uncertainties in Mexico City during MILAGRO-2006 field campaign, *Atmos. Chem. Phys.*, 12, 11295–11308, doi:10.5194/acp-12-11295-2012, 2012.
- Brasseur, G. P., Orlando, J. J., and Tyndall, G. S.: *Atmospheric chemistry and global change*, Oxford University Press, Cambridge, USA, 654 p., 1999.
- 15 Cao, J. J., Wu, F., Chow, J. C., Lee, S. C., Li, Y., Chen, S. W., An, Z. S., Fung, K. K., Watson, J. G., Zhu, C. S., and Liu, S. X.: Characterization and source apportionment of atmospheric organic and elemental carbon during fall and winter of 2003 in Xi'an, China, *Atmos. Chem. Phys.*, 5, 3127–3137, doi:10.5194/acp-5-3127-2005, 2005.
- 20 Cao, J., Xu, H., Xu, Q., Chen, B., and Kan, H.: Fine particulate matter constituents and cardiopulmonary mortality in a heavily polluted Chinese city, *Environ. Health Persp.*, 120, 373–378, 2012.
- Castro, T., Madronich, S., Rivale, S., Muhlia, A., and Mar, B.: The influence of aerosols on photochemical smog in Mexico City, *Atmos. Environ.*, 35, 1765–1772, 2001.
- Chen, F. and Dudhia, J.: Coupling an advanced land-surface/hydrology model with the Penn State/NCARMM5modelingsystem. Part I: Model description and implementation, *Mon. Weather Rev.*, 129, 569–585, 2001.
- 25 Cheng, H. R., Guo, H., Saunders, S. M., Lam, S. H. M., Jiang, F., Wang, X. M., Simpson, I. J., Blake, D. R., Louie, P. K. K., and Wang, T. J.: Assessing photochemical ozone formation in the Pearl River Delta with a photochemical trajectory model, *Atmos. Environ.*, 44, 4199–4208, 30 2010.

## Summertime ozone formation in Xi'an and surrounding areas, China

T. Feng et al.

Title Page

Abstract

Introduction

Conclusions

References

Tables

Figures



Back

Close

Full Screen / Esc

Printer-friendly Version

Interactive Discussion





**Summertime ozone formation in Xi'an and surrounding areas, China**

T. Feng et al.

Title Page

Abstract

Introduction

Conclusions

References

Tables

Figures



Back

Close

Full Screen / Esc

Printer-friendly Version

Interactive Discussion



Li, G., Bei, N., Tie, X., and Molina, L. T.: Aerosol effects on the photochemistry in Mexico City during MCMA-2006/MILAGRO campaign, *Atmos. Chem. Phys.*, 11, 5169–5182, doi:10.5194/acp-11-5169-2011, 2011a.

Li, G., Zavala, M., Lei, W., Tsimpidi, A. P., Karydis, V. A., Pandis, S. N., Canagaratna, M. R., and Molina, L. T.: Simulations of organic aerosol concentrations in Mexico City using the WRF-CHEM model during the MCMA-2006/MILAGRO campaign, *Atmos. Chem. Phys.*, 11, 3789–3809, doi:10.5194/acp-11-3789-2011, 2011b.

Li, G., Lei, W., Bei, N., and Molina, L. T.: Contribution of garbage burning to chloride and PM<sub>2.5</sub> in Mexico City, *Atmos. Chem. Phys.*, 12, 8751–8761, doi:10.5194/acp-12-8751-2012, 2012.

Lin, W., Xu, X., Zhang, X., and Tang, J.: Contributions of pollutants from North China Plain to surface ozone at the Shangdianzi GAW Station, *Atmos. Chem. Phys.*, 8, 5889–5898, doi:10.5194/acp-8-5889-2008, 2008.

Lin, Y.-L., Farley, R. D., and Orville, H. D.: Bulk parameterization of the snow field in a cloud model, *J. Appl. Meteorol.*, 22, 1065–1092, 1983.

Lu, Z., Zhang, Q., and Streets, D. G.: Sulfur dioxide and primary carbonaceous aerosol emissions in China and India, 1996–2010, *Atmos. Chem. Phys.*, 11, 9839–9864, doi:10.5194/acp-11-9839-2011, 2011.

Mlawer, E. J., Taubman, S. J., Brown, P. D., Iacono, M. J., and Clough, S. A.: Radiative transfer for inhomogeneous atmosphere: RRTM, a validated correlated-k model for the long-wave J. *Geophys. Res.*, 102, 16663–16682, 1997.

Seinfeld, J. H. and Pandis, S. N.: *Atmospheric chemistry and physics: from air pollution to climate Change*, 2nd Edition, John Wiley & Sons, Inc., New York, USA, 1326 p., 2006.

Shen, Z. X., Arimoto, R., Okuda, T., Cao, J. J., Zhang, R. J., Li, X. X., Du, N., Nakao, S., and Tanaka, S.: Seasonal variations and evidence for the effectiveness of pollution controls on water-soluble inorganic species in TSP and PM<sub>2.5</sub> from Xi'an, China, *J. Air Waste Manage.*, 58, 1560–1570, 2008.

Shen, Z., Cao, J., Arimoto, R., Han, Z., Zhang, R., Han, Y., Liu, S., Okuda, T., Nakao, S., and Tanaka, S.: Ionic composition of TSP and PM<sub>2.5</sub> during dust storms and air pollution episodes at Xi'an, China, *Atmos. Environ.*, 43, 2911–2918, 2009.

Shrivastava, M. K., Lane, T. E., Donahue, N. M., Pandis, S. N., and Robinson, A. L.: Effects of gas-particle partitioning and aging of primary emissions on urban and regional organic aerosol concentrations, *J. Geophys. Res.*, 113, D18301, doi:10.1029/2007JD009735, 2008.

## Summertime ozone formation in Xi'an and surrounding areas, China

T. Feng et al.

Title Page

Abstract

Introduction

Conclusions

References

Tables

Figures



Back

Close

Full Screen / Esc

Printer-friendly Version

Interactive Discussion



- Sillman, S.: The use of  $\text{NO}_y$ ,  $\text{H}_2\text{O}_2$  and  $\text{HNO}_3$  as indicators for  $\text{O}_3$ - $\text{NO}_x$ -VOC sensitivity in urban locations, *J. Geophys. Res.*, 100, 14175–14188, 1995.
- Skamarock, W. C.: Evaluating Mesoscale NWP models using kinetic energy spectra, *Mon. Weather Rev.*, 132, 3019–3032, 2004.
- 5 Stockwell, W. R. and Goliff, W. S.: Measurement of actinic flux and the calculation of photolysis rate parameters for the Central California Ozone Study, *Atmos. Environ.*, 38, 5169–5177, 2004.
- Su, X., Cao, J., Li, Z., Lin, M., and Wang, G.: Column-integrated aerosol optical properties during summer and autumn of 2012 in Xi'an, China, *Aerosol Air Qual. Res.*, 14, 850–861, doi:10.4209/aaqr.2013.03.0093, 2014.
- 10 Tang, G., Li, X., Wang, Y., Xin, J., and Ren, X.: Surface ozone trend details and interpretations in Beijing, 2001–2006, *Atmos. Chem. Phys.*, 9, 8813–8823, doi:10.5194/acp-9-8813-2009, 2009.
- Tie, X., Madronich, S., Walters, S., Zhang, R., Rasch, P., and Collins, W.: Effect of clouds on photolysis and oxidants in the troposphere, *J. Geophys. Res.*, 108, 4642, doi:10.1029/2003JD003659, 2003.
- Tie, X., Geng, F. H., Peng, L., Gao, W., and Zhao, C. S.: Measurement and modeling of  $\text{O}_3$  variability in Shanghai, China; Application of the WRF-CHEM model, *Atmos. Environ.*, 43, 4289–4302, 2009.
- 20 Tie, X., Geng, F., Guenther, A., Cao, J., Greenberg, J., Zhang, R., Apel, E., Li, G., Weinheimer, A., Chen, J., and Cai, C.: Megacity impacts on regional ozone formation: observations and WRF-Chem modeling for the MIRAGE-Shanghai field campaign, *Atmos. Chem. Phys.*, 13, 5655–5669, doi:10.5194/acp-13-5655-2013, 2013.
- Tsimpidi, A. P., Karydis, V. A., Zavala, M., Lei, W., Molina, L., Ulbrich, I. M., Jimenez, J. L., and Pandis, S. N.: Evaluation of the volatility basis-set approach for the simulation of organic aerosol formation in the Mexico City metropolitan area, *Atmos. Chem. Phys.*, 10, 525–546, doi:10.5194/acp-10-525-2010, 2010.
- 25 Volkamer, R., San Martini, F., Molina, L. T., Salcedo, D., Jimenez, J. L., and Molina, M. J.: A Missing Sink for Gas-Phase Glyoxal in Mexico City: Formation of Secondary Organic Aerosol, *Geophys. Res. Lett.*, 34, L19807, doi:10.1029/2007GL030752, 2007.
- Wang, T., Ding, A., Gao, J., and Wu, W. S.: Strong ozone production in urban plumes from Beijing, China, *Geophys. Res. Lett.*, 33, L21806, doi:10.1029/2006GL027689, 2006.

**Summertime ozone formation in Xi'an and surrounding areas, China**

T. Feng et al.

Title Page

Abstract

Introduction

Conclusions

References

Tables

Figures



Back

Close

Full Screen / Esc

Printer-friendly Version

Interactive Discussion



- Wang, T., Wei, X. L., Ding, A. J., Poon, C. N., Lam, K. S., Li, Y. S., Chan, L. Y., and Anson, M.: Increasing surface ozone concentrations in the background atmosphere of Southern China, 1994–2007, *Atmos. Chem. Phys.*, 9, 6217–6227, doi:10.5194/acp-9-6217-2009, 2009.
- 5 Wang, X., Zhang, Y., Hu, Y., Zhou, W., Zeng, L., Hu, M., Cohan, D. S., and Russell, A. G.: Decoupled direct sensitivity analysis of regional ozone pollution over the Pearl River Delta during the PRIDE-PRD2004 campaign, *Atmos. Environ.*, 45, 4941–4949, 2011.
- Wang, X., Shen, Z., Cao, J., Zhang, L., Liu, L., Li, J., Liu, L., and Sun, Y.: Characteristics of surface ozone at an urban site of Xi'an in Northwest China, *J. Environ. Monit.*, 14, 116–125, 2012.
- 10 Xu, J., Ma, J. Z., Zhang, X. L., Xu, X. B., Xu, X. F., Lin, W. L., Wang, Y., Meng, W., and Ma, Z. Q.: Measurements of ozone and its precursors in Beijing during summertime: impact of urban plumes on ozone pollution in downwind rural areas, *Atmos. Chem. Phys.*, 11, 12241–12252, doi:10.5194/acp-11-12241-2011, 2011.
- Zhang, Q., Streets, D. G., Carmichael, G. R., He, K. B., Huo, H., Kannari, A., Klimont, Z., Park, I. S., Reddy, S., Fu, J. S., Chen, D., Duan, L., Lei, Y., Wang, L. T., and Yao, Z. L.: Asian emissions in 2006 for the NASA INTEX-B mission, *Atmos. Chem. Phys.*, 9, 5131–5153, doi:10.5194/acp-9-5131-2009, 2009.
- 15 Zhang, Y. H., Su, H., Zhong, L. J., Cheng, Y. F., Zeng, L. M., Wang, X. S., Xiang, Y. R., Wang, J. L., Gao, D. F., and Shao, M.: Regional ozone pollution and observation-based approach for analyzing ozone–precursor relationship during the PRIDE-PRD2004 campaign, *Atmos. Environ.*, 42, 6203–6218, 2008.
- Zhao, J., Levitt, N. P., Zhang, R. Y., and Chen, J. M.: Heterogeneous reactions of methylglyoxal in acidic media: implications for secondary organic aerosol formation, *Environ. Sci. Technol.*, 40, 7682–7687, 2006.
- 20 Zhou, J., Ito, K., Lall, R., Lippmann, M., and Thurston, G.: Time-series analysis of mortality effects of fine particulate matter components in Detroit and Seattle, *Environ. Health Persp.*, 119, 461–466, 2011.

## Summertime ozone formation in Xi'an and surrounding areas, China

T. Feng et al.

Title Page

Abstract

Introduction

Conclusions

References

Tables

Figures

◀

▶

◀

▶

Back

Close

Full Screen / Esc

Printer-friendly Version

Interactive Discussion



**Table 1.** Statistical comparison of simulated and measured  $O_3$ ,  $NO_2$ ,  $PM_{2.5}$ , temperature, relative humidity, and wind speed at monitoring sites from 22 to 24 August 2013.

Predictands	Classification	MB	RMSE	IOA
$O_3$ ( $\mu\text{g m}^{-3}$ )	Averaged	−9.0	29.	0.91
$NO_2$ ( $\mu\text{g m}^{-3}$ )	Averaged	−5.2	11.	0.73
$PM_{2.5}$ ( $\mu\text{g m}^{-3}$ )	Averaged	−1.4	21.	0.92
Temperature ( $^{\circ}\text{C}$ )	Averaged	−0.76	1.1	0.97
Relative humidity (%)	Averaged	−4.5	5.5	0.92
Wind speed ( $\text{m s}^{-1}$ )	Xi'an	1.7	2.1	0.26
	Xianyang	1.3	1.5	0.61
	Jinghe	0.14	1.1	0.74
	Lintong	1.2	1.5	0.63
	Chang'an	0.69	1.2	0.47
	Lantian	0.43	1.1	0.61

## Summertime ozone formation in Xi'an and surrounding areas, China

T. Feng et al.

Title Page

Abstract

Introduction

Conclusions

References

Tables

Figures

◀

▶

◀

▶

Back

Close

Full Screen / Esc

Printer-friendly Version

Interactive Discussion



**Table 2.** Occurrence days of the defined  $\text{PM}_{2.5}$  and  $\text{O}_3$  exceedance levels during 2013 summertime.

	Beijing	Tianjin	Shijiazhuang	Ji'nan	Taiyuan	Xi'an
Level I <sup>a</sup>	57	65	64	72	53	61
Level II <sup>b</sup>	33	41	43	41	28	20

<sup>a</sup> hourly  $\text{PM}_{2.5}$  and  $\text{O}_3$  concentrations exceeding 35 and  $160 \mu\text{g m}^{-3}$ , respectively

<sup>b</sup> hourly  $\text{PM}_{2.5}$  and  $\text{O}_3$  concentrations exceeding 75 and  $200 \mu\text{g m}^{-3}$ , respectively

## Summertime ozone formation in Xi'an and surrounding areas, China

T. Feng et al.

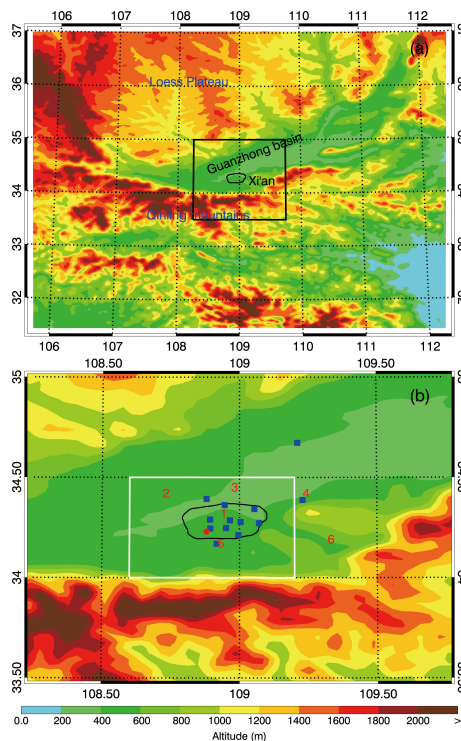


**Figure 1.** (a) WRF-CHEM model simulation domain with topography and (b) geographic distributions of surface monitoring stations. In (b), the blue squares represent the chemical species monitoring stations and the red circle is the IEECAS site. The red numbers denote meteorological observation sites. 1: Xi'an; 2: Xianyang; 3: Jinghe; 4: Lintong; 5: Chang'an; 6: Lantian. In addition, the area surrounded by the white rectangle in (b) is defined as Xi'an and surrounding areas according to the plume movement, and the area surrounded by the black line is the urban region of Xi'an.

[Title Page](#)
[Abstract](#)
[Introduction](#)
[Conclusions](#)
[References](#)
[Tables](#)
[Figures](#)
[Back](#)
[Close](#)
[Full Screen / Esc](#)
[Printer-friendly Version](#)
[Interactive Discussion](#)



## Summertime ozone formation in Xi'an and surrounding areas, China

T. Feng et al.

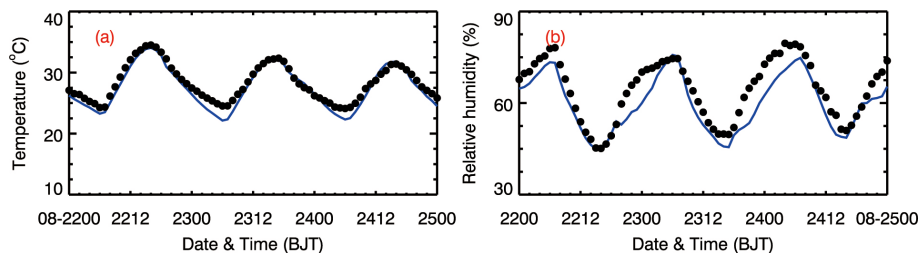


**Figure 3.** Observed (black dots) and simulated (blue lines) diurnal profiles of **(a)** surface temperature and **(b)** relative humidity averaged over six meteorological sites from 22 to 24 August 2013.

[Title Page](#)[Abstract](#)[Introduction](#)[Conclusions](#)[References](#)[Tables](#)[Figures](#)[◀](#)[▶](#)[◀](#)[▶](#)[Back](#)[Close](#)[Full Screen / Esc](#)[Printer-friendly Version](#)[Interactive Discussion](#)

## Summertime ozone formation in Xi'an and surrounding areas, China

T. Feng et al.

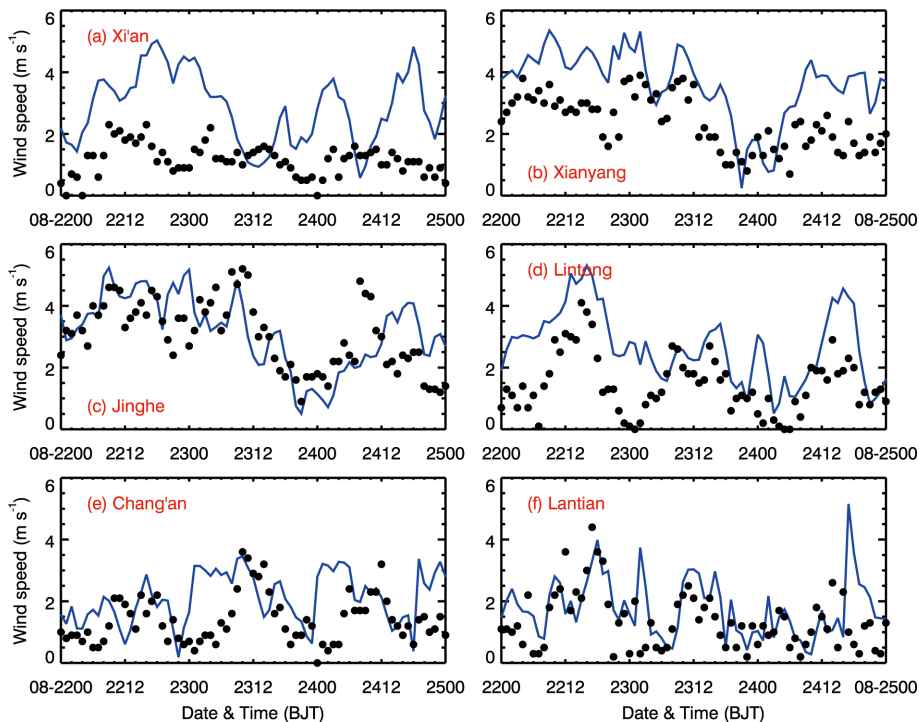


**Figure 4.** Observed (black dots) and simulated (blue lines) diurnal profiles of surface wind speeds at six meteorological sites from 22 to 24 August 2013.

[Title Page](#)[Abstract](#)[Introduction](#)[Conclusions](#)[References](#)[Tables](#)[Figures](#)[Back](#)[Close](#)[Full Screen / Esc](#)[Printer-friendly Version](#)[Interactive Discussion](#)

Summertime ozone formation in Xi'an and surrounding areas, China

T. Feng et al.

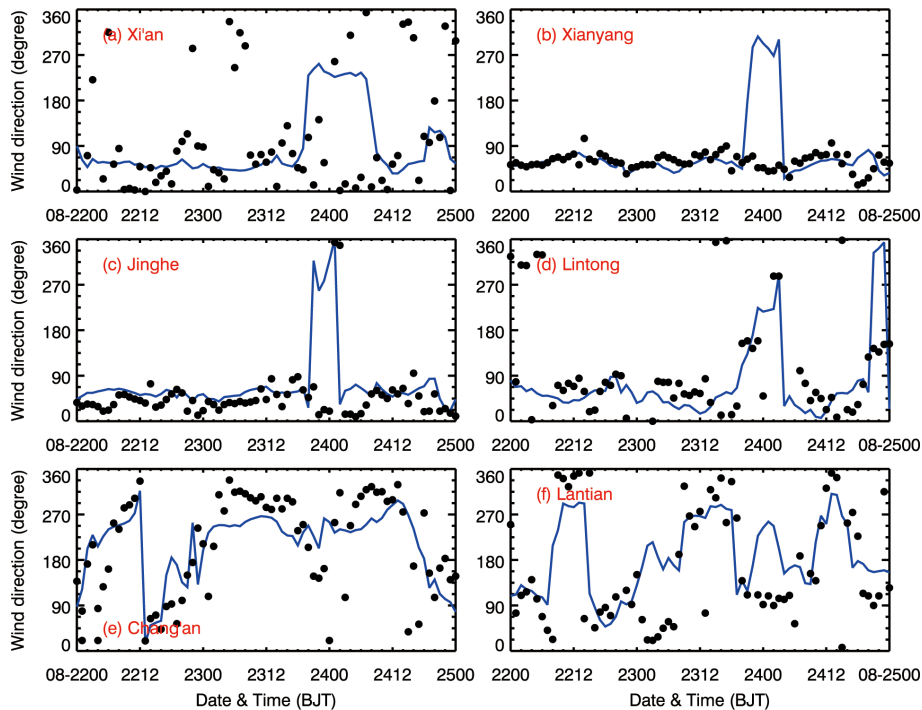


Figure 5. Same as Fig. 4, but for surface wind directions.

Title Page

Abstract Introduction

Conclusions References

Tables Figures

◀ ▶

◀ ▶

Back Close

Full Screen / Esc

Printer-friendly Version

Interactive Discussion



## Summertime ozone formation in Xi'an and surrounding areas, China

T. Feng et al.

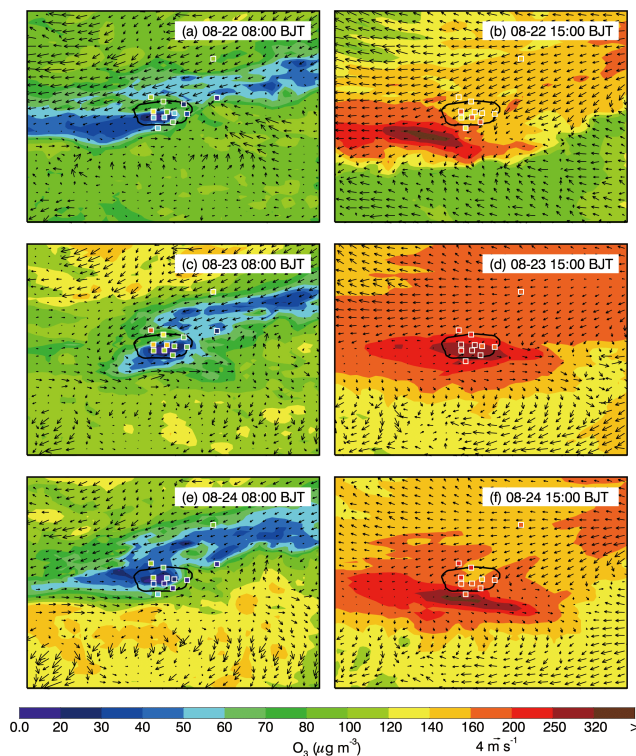


**Figure 6.** Pattern comparison of simulated vs. observed near-surface  $O_3$  concentrations at 08:00 and 15:00 BJT from 22 to 24 August 2013. Colored squares:  $O_3$  observations; color contour:  $O_3$  simulations; black arrows: simulated surface winds.

Title Page

Abstract

Introduction

Conclusions

References

Tables

Figures

◀

▶

◀

▶

Back

Close

Full Screen / Esc

Printer-friendly Version

Interactive Discussion



## Summertime ozone formation in Xi'an and surrounding areas, China

T. Feng et al.

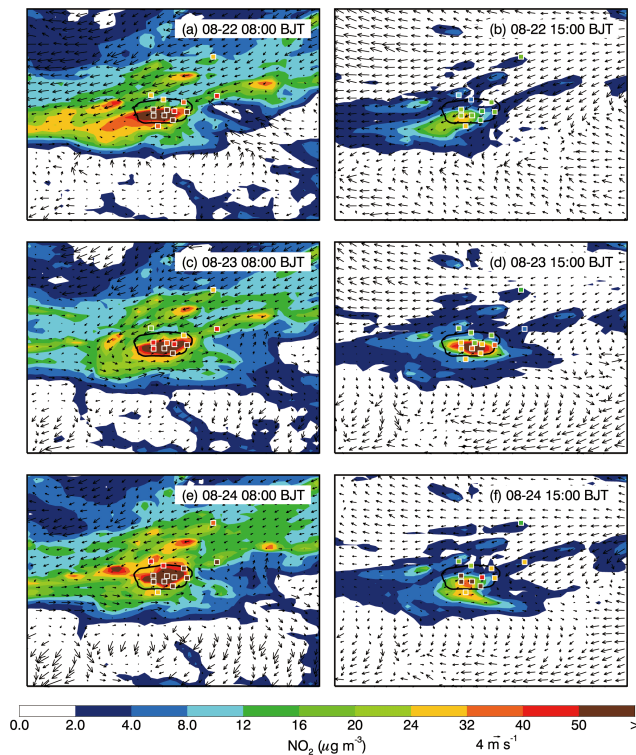


Figure 7. Same as Fig. 6, but for NO<sub>2</sub>.

[Title Page](#)[Abstract](#)[Introduction](#)[Conclusions](#)[References](#)[Tables](#)[Figures](#)[◀](#)[▶](#)[◀](#)[▶](#)[Back](#)[Close](#)[Full Screen / Esc](#)[Printer-friendly Version](#)[Interactive Discussion](#)



Summertime ozone formation in Xi'an and surrounding areas, China

T. Feng et al.

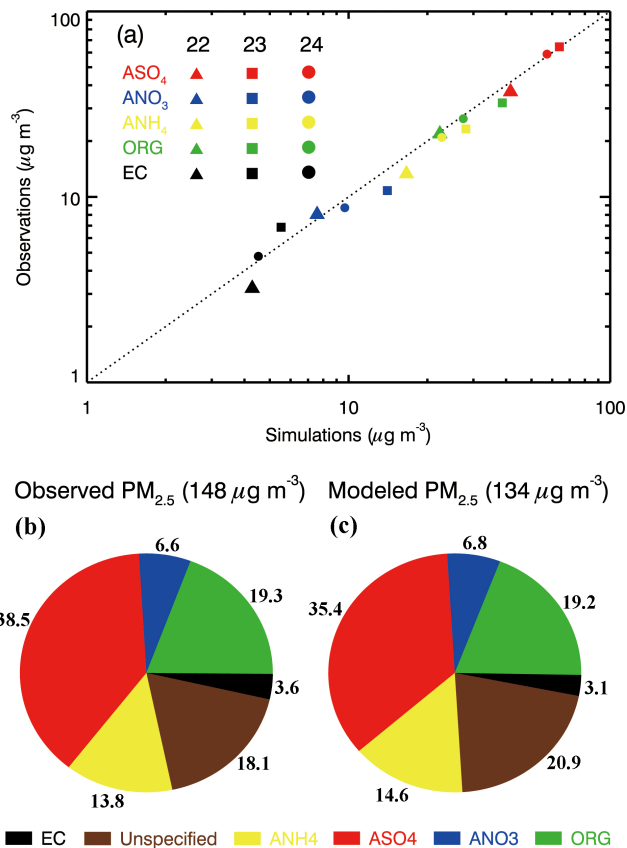


**Figure 9.** (a) scattering plot of measured daily aerosol constituents with simulations and comparison of (b) measured and (c) modeled  $\text{PM}_{2.5}$  chemical composition (%).

Title Page

Abstract Introduction

Conclusions References

Tables Figures

◀ ▶

◀ ▶

Back Close

Full Screen / Esc

Printer-friendly Version

Interactive Discussion



## Summertime ozone formation in Xi'an and surrounding areas, China

T. Feng et al.

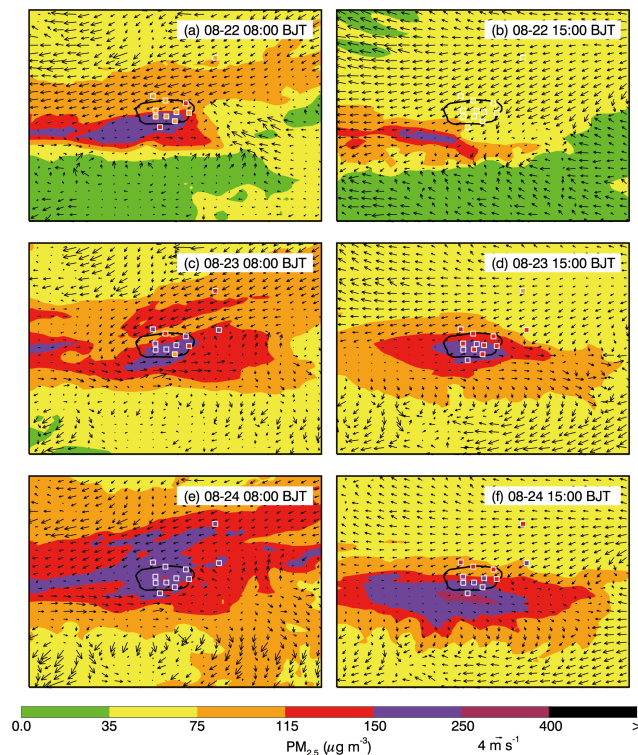


Figure 10. Same as Fig. 6, but for PM<sub>2.5</sub>.

[Title Page](#)[Abstract](#)[Introduction](#)[Conclusions](#)[References](#)[Tables](#)[Figures](#)[◀](#)[▶](#)[◀](#)[▶](#)[Back](#)[Close](#)[Full Screen / Esc](#)[Printer-friendly Version](#)[Interactive Discussion](#)

## Summertime ozone formation in Xi'an and surrounding areas, China

T. Feng et al.

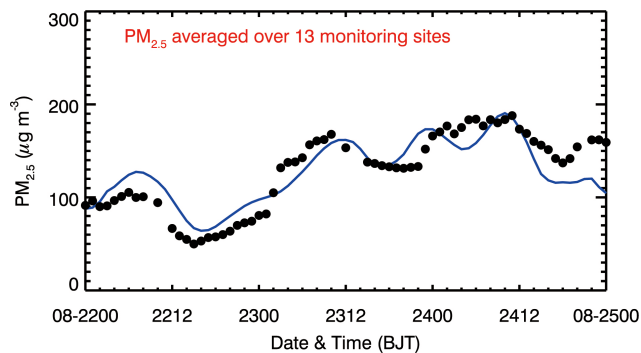
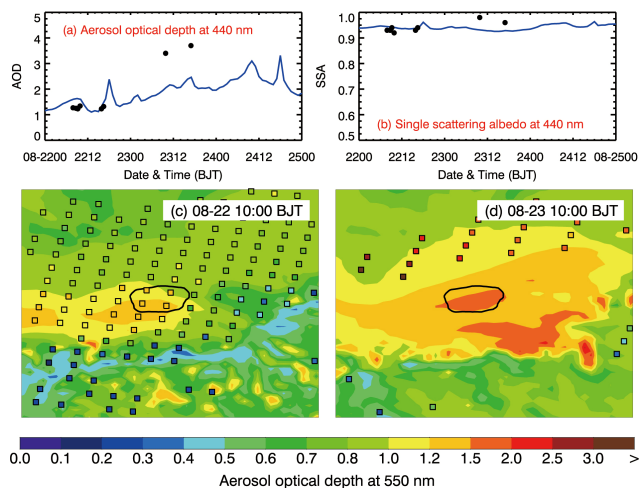


Figure 11. Same as Fig. 8, but for  $PM_{2.5}$ .

[Title Page](#)[Abstract](#)[Introduction](#)[Conclusions](#)[References](#)[Tables](#)[Figures](#)[◀](#)[▶](#)[◀](#)[▶](#)[Back](#)[Close](#)[Full Screen / Esc](#)[Printer-friendly Version](#)[Interactive Discussion](#)

## Summertime ozone formation in Xi'an and surrounding areas, China

T. Feng et al.



**Figure 12.** Retrieved (black dots) and calculated (blue lines) diurnal profiles of **(a)** AOD and **(b)** aerosol SSA at 440 nm at IEECAS site from 22 to 24 August 2013, and pattern comparison of calculated vs. retrieved AOD at 550 nm at 10:00 BJT **(c)** on 22 August and **(d)** 23 August 2013. Colored squares: retrieved AOD; color contour: calculated AOD.

## Summertime ozone formation in Xi'an and surrounding areas, China

T. Feng et al.

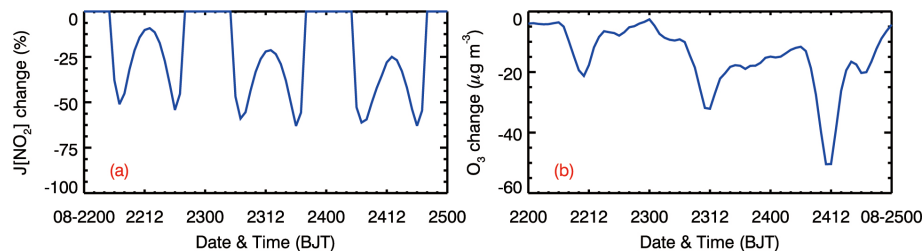


**Figure 13.** Diurnal variations of the change of (a)  $J[\text{NO}_2]$  and (b)  $\text{O}_3$  concentrations averaged in Xi'an and surrounding areas due to aerosol effects from 22 to 24 August 2013.

[Title Page](#)[Abstract](#)[Introduction](#)[Conclusions](#)[References](#)[Tables](#)[Figures](#)[◀](#)[▶](#)[◀](#)[▶](#)[Back](#)[Close](#)[Full Screen / Esc](#)[Printer-friendly Version](#)[Interactive Discussion](#)

## Summertime ozone formation in Xi'an and surrounding areas, China

T. Feng et al.

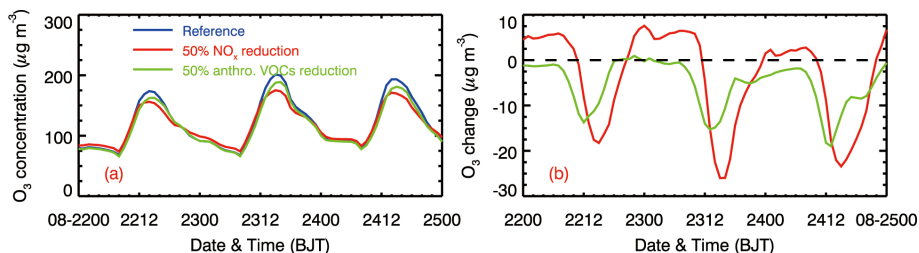


**Figure 14.** Diurnal profiles of **(a)** O<sub>3</sub> concentrations and **(b)** O<sub>3</sub> changes averaged in Xi'an and surrounding areas caused by a 50% reduction of anthropogenic NO<sub>x</sub> and VOCs emissions, respectively, from 22 to 24 August 2013. Blue line: the reference simulation; red line: the simulation with a 50% reduction of anthropogenic NO<sub>x</sub> emissions; green line: the simulation with a 50% reduction of anthropogenic VOCs emissions.

[Title Page](#)[Abstract](#)[Introduction](#)[Conclusions](#)[References](#)[Tables](#)[Figures](#)[◀](#)[▶](#)[◀](#)[▶](#)[Back](#)[Close](#)[Full Screen / Esc](#)[Printer-friendly Version](#)[Interactive Discussion](#)

## Summertime ozone formation in Xi'an and surrounding areas, China

T. Feng et al.

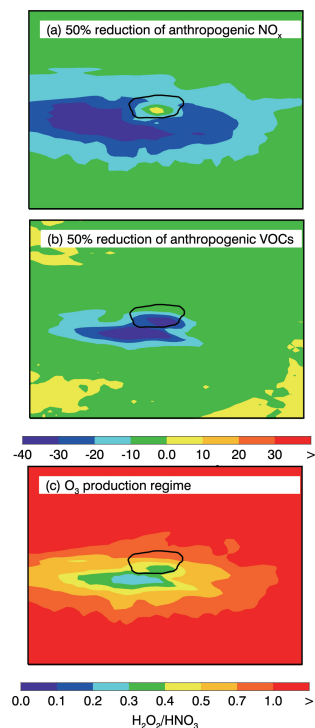


**Figure 15.** Change of  $\text{O}_3$  concentrations in the bottom model layer, averaged during  $\text{O}_3$  peak time from 22 to 24 August 2013 due to a 50% reduction of anthropogenic (a)  $\text{NO}_x$  and (b) VOCs emissions, and (c) the 3-day average ratio of  $\text{H}_2\text{O}_2/\text{HNO}_3$  during  $\text{O}_3$  peak time.

**Summertime ozone formation in Xi'an and surrounding areas, China**

T. Feng et al.

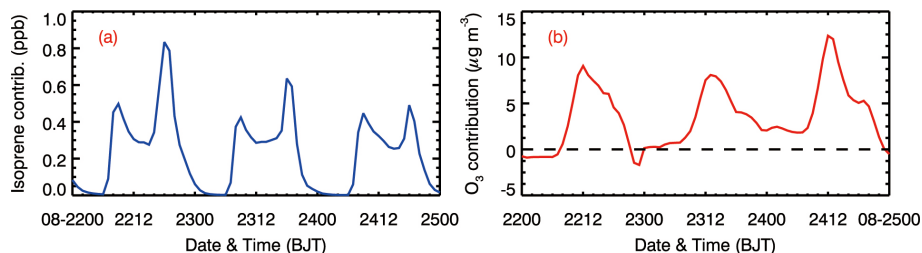


**Figure 16.** Diurnal variations of contributions of biogenic emissions to near-surface isoprene and O<sub>3</sub> concentrations averaged in Xi'an and surrounding areas from 22 to 24 August 2013.

[Title Page](#)[Abstract](#)[Introduction](#)[Conclusions](#)[References](#)[Tables](#)[Figures](#)[◀](#)[▶](#)[◀](#)[▶](#)[Back](#)[Close](#)[Full Screen / Esc](#)[Printer-friendly Version](#)[Interactive Discussion](#)

## Summertime ozone formation in Xi'an and surrounding areas, China

T. Feng et al.

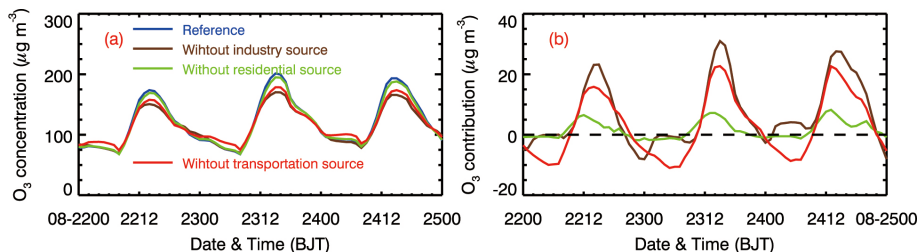


**Figure 17.** Diurnal profiles of **(a)** O<sub>3</sub> concentrations and **(b)** O<sub>3</sub> contribution from various anthropogenic sources averaged in Xi'an and surrounding areas from 22 to 24 August 2013. Blue line: the reference simulation; brown line: the simulation without industry emissions; green line: the simulation without residential emissions; red line: the simulation without transportation emissions.

[Title Page](#)[Abstract](#)[Introduction](#)[Conclusions](#)[References](#)[Tables](#)[Figures](#)[◀](#)[▶](#)[◀](#)[▶](#)[Back](#)[Close](#)[Full Screen / Esc](#)[Printer-friendly Version](#)[Interactive Discussion](#)

## Summertime ozone formation in Xi'an and surrounding areas, China

T. Feng et al.

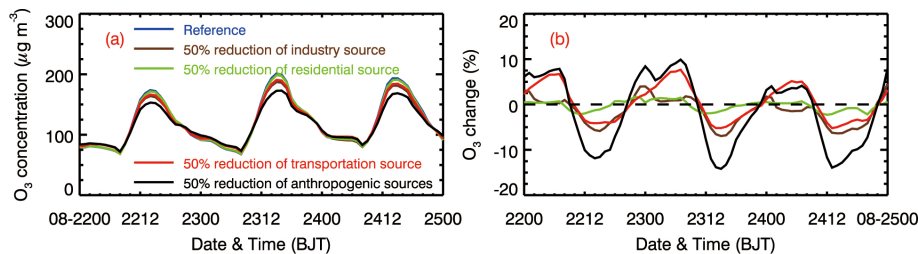


**Figure 18.** Diurnal profiles of **(a)** O<sub>3</sub> concentrations and **(b)** O<sub>3</sub> changes averaged in Xi'an and surrounding areas caused by a 50 % reduction of various anthropogenic sources from 22 to 24 August 2013. Blue line: the reference simulation; brown line: the simulation with a 50 % reduction of industry emissions; green line: the simulation with a 50 % reduction of residential emissions; red line: the simulation with a 50 % reduction of transportation emissions; the black line: the simulation with a 50 % of all anthropogenic emissions.

[Title Page](#)[Abstract](#)[Introduction](#)[Conclusions](#)[References](#)[Tables](#)[Figures](#)[◀](#)[▶](#)[◀](#)[▶](#)[Back](#)[Close](#)[Full Screen / Esc](#)[Printer-friendly Version](#)[Interactive Discussion](#)